Journal of Inorganic and General Chemistry
ZAAC
Zeitschrift für anorganische und allgemeine Chemie
DOI: 10.1002/zaac.201900222
ARTICLE

Synthesis and Characterisation of the Nitridocuprate(I) Nitride Carbodiimide $(Sr_6N)[CuN_2][CN_2]_2$

William P. Clark[a] and Rainer Niewa*[a]

Dedicated to Professor Hans-Jörg Deiseroth on the Occasion of his 75th Birthday

Abstract. The strontium nitridocuprate(I) nitride carbodiimide has been successfully produced and characterised. Single crystals were grown in metal ampoules, utilising an alkali metal as a fluxing agent. Structural characterisation was conducted via single-crystal X-ray diffraction and the identity of the $[CN_2]^{2-}$ anion as carbodiimide was confirmed by Raman spectroscopy. Diamagnetic behaviour over a large temperature range supports the copper(I) electronic state.

Introduction

The pseudo-chalcogenide anion $[CN_2]^{2-}$ was first discovered in the compound $Ca[CN_2]$[1] and its compounds have since grown into a family, that has been intensely studied. The $[CN_2]^{2-}$ anion exists as either the symmetric carbodiimide anion, $[N{=}C{=}N]^{2-}$, or the asymmetric cyanamide, $[N{\equiv}C{-}N]^{2-}$ The determining factor of which of the two forms is favoured is caused by the cations present. The symmetric, near linear carbodiimide anion $[N{=}C{=}N]^{2-}$ tends to form in the presence of hard cations, due to the preferred ionic character. Whereas, the near linear cyanamide anion $[N{\equiv}C{-}N]^{2-}$ rather arises in the presence of soft cations, since these cations have a stronger preference to covalent bond to one side of the anion, resulting in the asymmetric cyanamide unit.

Many binary carbodiimides, such as $M[CN_2]$ (M = Mg – Ba and Eu),[1–4] $Cr_2[CN_2]_3$[5] and $M[CN_2]$ (M = Mn – Zn),[6–10] as well as binary cyanamides, such as $M[CN_2]$ (M = Cd and Pb),[11,12] have been previously reported. For M = Hg two modifications, one cyanamide and one carbodiimide, are known.[13,14] Interestingly, some of these compounds show potential applications as negative electrode materials for lithium and sodium ion batteries,[15–19] corrosion protective layers,[20] photovoltaic devices,[21] fluorescent light sources[22,23] and light-emitting diodes.[24,25] Due to the carbodiimide anion being a pseudo-chalcogenide anion, it can act as a bridging ligand to allow effective magnetic super exchange between bridged paramagnetic cations, as seen for $Cr_2[CN_2]_3$ and $M[CN_2]$ (M = Mn – Cu), which are isostructural to their respective oxide variants, exhibit similar magnetic ordering and also have the same colours.[5–9] This ability of the carbodiimide anion has also made it an interesting field of investigation for new magnetic materials.

Nitridocuprates(I) of alkaline earth metals, on the other hand, typically contain similar three-atomic near linear units $[CuN_2]^{5-}$, or condensation products thereof, leading to infinite chains or chain fragments.[26] Interestingly, such linear coordination, frequently in combination with an oxidation state of +1 for the transition metal, is also the dominating structural motif for respective nitridometalates of Ni, Co, Fe, and Mn.

As mentioned previously, transition metal cations can function as the counter cation for the $[CN_2]^{2-}$ anion. However, the transition metal can also act as part of a complex anion alongside the $[CN_2]^{2-}$ anion. Compounds of such type, constituting from carbodiimide anions next to nitridometalate anions, with the form $[MN_x]^{y-}$, have been reported for several 3d, 4d and 5d transition metals in $Sr_6[CoN_2]_2[CN_2]$, $(Sr_6N)[MN_2][CN_2]_2$ (M = Fe, Co), $Ba_8[MN_4][CN_2]_5$ and $(Ba_6N)_2[MN_4][CN_2]_6$ (M = Mo and W), and $Ba_9[MN_4]O[CN_2]$ (M = Ta and Nb).[26–31] Recent research has also revealed that nitridometalates are structurally more diverse than previously thought.[32]

Herein, we report the production of $(Sr_6N)[CuN_2][CN_2]_2$, which was characterized by single-crystal X-ray diffraction, Raman spectroscopy and elemental analysis.

Results and Discussion

Synthetic Considerations

Synthesis of the titular compound was performed in a two-step reaction, essentially from the ternary nitridocuprate $Li_2[(Li_{1-x}Cu_x)N]$ with elemental carbon and strontium. However, as can be taken from literature, such compounds similarly may form directly from the elements.[27,28] During synthesis in a sealed metal ampoule, excess sodium was used as fluxing

* Prof. Dr. R. Niewa
E-Mail: rainer.niewa@iac.uni-stuttgart.de
[a] Institut für Anorganische Chemie
Universität Stuttgart
Pfaffenwaldring 55
70569 Stuttgart, Germany
Supporting information for this article is available on the WWW under **http://dx.doi.org/10.1002/zaac.201900222** or from the author.

agent to aid crystal growth. Sodium presents an ideal flux for nitride synthesis, since it does not form a binary nitride stable under the synthesis conditions and is rarely observed to take part in ternary nitride formation.[33] Additionally, alkaline earth metals such as strontium are discussed to markedly increase the solubility of nitrogen in liquid sodium.[34] Particularly for crystal growth of alkaline earth metal nitridocuprates, this fluxing agent was shown to be successful, in the past.[35]

Crystal Structure Determination

X-ray diffraction intensity data were collected on a rectangular red single crystal and the resulting refinements of the structural data showed that the compound crystallises in the space group $P2_1/c$ (No. 14), with the composition of $(Sr_6N)[CuN_2][CN_2]_2$ (Table 1, Tables S1 and S2, Supporting Information).

Table 1. Selected data for the crystal structure refinements for $(Sr_6N)[CuN_2][CN_2]_2$.

	$(Sr_6N)[CuN_2][CN_2]_2$
Crystal system	monoclinic
Space group	$P2_1/c$ (no. 14)
Z	2
a /Å	3.8454(1)
b /Å	9.9244(3)
c /Å	14.6528(5)
β /°	92.280(2)
ρ_{calc} /g·cm^{-3}	4.228
Volume V /Å^3	558.76
Measurement temperature /K	293(2)
Index range	$-4 \le h \le 4$
	$-12 \le k \le 12$
	$-18 \le l \le 18$
Max. 2θ /deg	54.99
F(000)	636.0
μ /mm^{-1}	30.26
Observed reflections	13782
Unique reflections	1265
Refined parameters	77
R_{int}/R_σ	0.0747/0.0309
R_1/wR_2	0.0300/0.0683
GooF	1.110
Remaining electron density (max / min) /Å^{-3}	1.07 / –1.32

Confirmation of the proposed $[CN_2]^{2-}$ unit and its discrimination from related (near) linear three-atomic ions, for example $[BN_2]^{3-}$ or $[C_2N]^{3-}$,[36–39] is not possible through the use of X-ray diffraction alone, however, the crystal structure is near identical to the previously reported carbodiimides $(Sr_6N)[MN_2][CN_2]_2$ (M = Fe, Co).[27,28] In addition, the C–N interatomic distances in the proposed $[CN_2]^{2-}$ anion [1.225(9) and 1.242(9) Å], are in very good agreement with those found in the previously reported phases, $(Sr_6N)[FeN_2][CN_2]_2$ (1.23 and 1.24 Å)[28] and $(Sr_6N)[CoN_2][CN_2]_2$ (1.23 and 1.24 Å).[27] Also, the C atoms showed a small anisotropic displacement parameter (Table S2, Supporting Information), implying that they are located in a symmetrical coordination environment. These facts served as a reasonable first indication that the three atom anions are indeed $[CN_2]^{2-}$.

The crystal structure of $(Sr_6N)[CuN_2][CN_2]_2$ is constructed of face sharing corrugated layers (Figure 1). The first layer is built of edge and corner sharing bidisphenoid polyhedra of Sr cations. Within these polyhedra $[CN_2]^{2-}$ anions are located, where the two crystallographically different N atoms are separately coordinated by eight Sr cations (Figure 2). The second layer contains $[CuN_2]^{5-}$ units, which build up two corner sharing octahedra of Sr_5CuN, with N at the centre (Figure 2). These octahedra are linked to form a corrugated layer by edge sharing with Sr_6N units. Such structural motifs are also observed in $(Sr_6N)[MN_2][CN_2]_2$ (M = Fe, Co),[27,28] however, the N-centred Sr_5CuN octahedra are, for the produced compound, less distorted than those seen for $(Sr_6N)[MN_2][CN_2]_2$ (M = Fe, Co).[27,28]

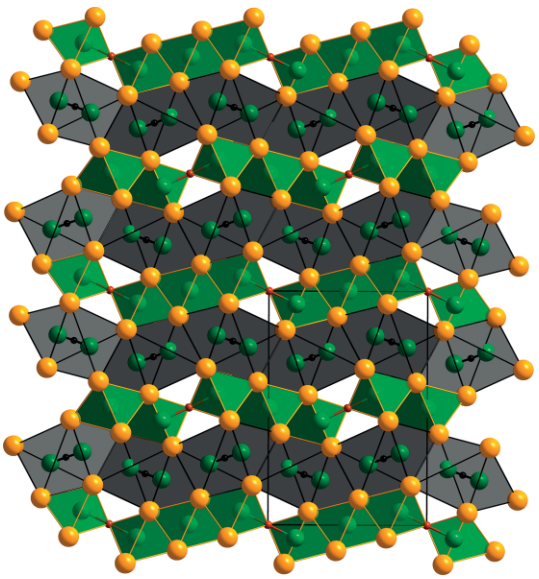

Figure 1. Section of the crystal structure of $(Sr_6N)[CuN_2][CN_2]_2$ viewed along [100]. Octahedral coordination polyhedra around nitride ions, N-ligands in $[CuN_2]^{5-}$ ions (both green) and N-ligands in carbodiimide ions (grey) are highlighted. Sr–orange, N–green, Cu–brown and C–black. Unit cell edges are shown by black lines.

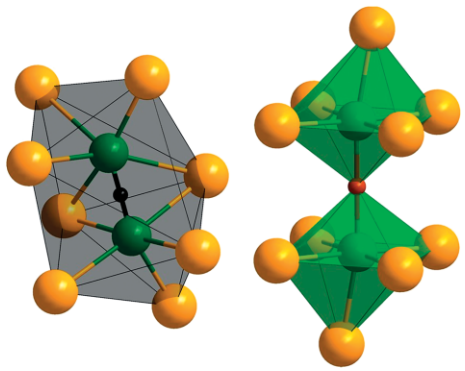

Figure 2. Coordination environments of $[CN_2]^{2-}$ (left) and $[CuN_2]^{5-}$ ions (right). Sr–orange, N–green, Cu–brown and C–black.

The linearly coordinated $[CuN_2]^{5-}$ anion shows a Cu–N interatomic distance of 1.899(5) Å, which is slightly longer than what has been previously seen for $[MN_2]^{5-}$ anions in

$(Sr_6N)[MN_2][CN_2]_2$ (M = Fe, Co), 1.85 Å and 1.84 Å respectively.[27,28] In addition the $[CuN_2]^{5-}$ units seen in the titular compound are linear (180(3)°], with the Cu–N interatomic distances being longer than those in linear $[MN_2]^{5-}$ anions of the other 3*d* metals, such as the distances seen in $Ca_4Ba[CuN_2]_2$ (1.865 Å)[35] with similar near linear [174(1)–179(1)°][35] isolated $[CuN_2]^{5-}$ ions. In general the Cu–N distance appears quite typical, when compared with the average interatomic distance (1.907 Å) seen for Cu_3N produced from various synthesis techniques.[40–42]

While the crystal structures of $(Sr_6N)[MN_2][CN_2]_2$ (M = Fe, Co) and the titular compound are extremely similar, they are not isostructural. The first indication of the difference is that both the Fe and Co variants crystallise in the orthorhombic space group $P2_12_12$ (No. 18), whereas $(Sr_6N)[CuN_2][CN_2]_2$ crystallises in the monoclinic space group $P2_1/c$ (No. 14). The only discernible difference appears to be that the $[CN_2]^{2-}$ anions for the iron and cobalt compounds are aligned, when viewed along [010], while they can be seen to "criss-cross" along the equivalent viewing direction [001] of the copper compound (Figure 3).

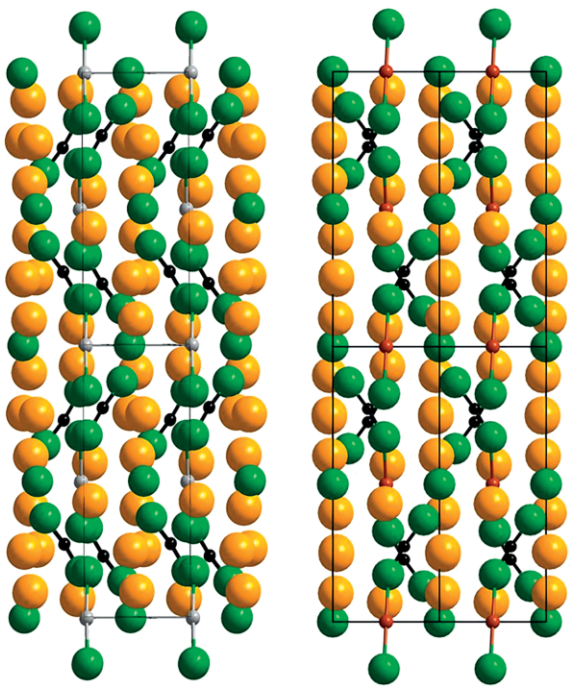

Figure 3. Comparison of sections of the crystal structures of $(Sr_6N)[MN_2][CN_2]_2$ (left),[27,28] viewed along [010] and $(Sr_6N)[CuN_2][CN_2]_2$ (right), viewed along [001]. Sr–orange, N–green, *M*–silver and Cu–brown. Unit cell edges are shown by black lines.

Several different approaches were used in an attempt to determine the cause for the difference in structures between $(Sr_6N)[MN_2][CN_2]_2$ (M = Fe, Co) and $(Sr_6N)[CuN_2][CN_2]_2$. Comparison of the synthesis methods showed the only difference was the cooling rate of 1 K·h^{-1}for the titular compound and a faster cooling rate of 10 K·h^{-1} for $(Sr_6N)[MN_2][CN_2]_2$ (M = Fe, Co).[27,28] This could imply that the monoclinic structure is in fact be the thermodynamic product and the orthorhombic structure was the kinetic product, however production of $(Sr_6N)[CuN_2][CN_2]_2$, with a faster cooling rate of 10 K·h^{-1}, still resulted in the monoclinic crystal system and the same "criss-cross" orientation of the $[CN_2]^{2-}$ units and thus showed that a different synthetic approach does not affect the resulting structure of the copper compound.

Since both previously reported compounds, $(Sr_6N)[MN_2][CN_2]_2$ (M = Fe, Co), contain paramagnetic transition metal cations, while the titular copper(I) compound, $(Sr_6N)[CuN_2][CN_2]_2$, contains a diamagnetic transition metal cation, a possible influence of magnetostriction had to be considered as cause for the structural difference between the otherwise very similar structures. If such an effect were present, then there should be a clear difference in the unit cell and axis ratios of $(Sr_6N)[MN_2][CN_2]_2$ (M = Fe, Co) and $(Sr_6N)[CuN_2][CN_2]_2$. This, however, is not the case, with the axis ratios of the monoclinic $(Sr_6N)[CuN_2][CN_2]_2$ being virtually identical to the equivalent axis ratios of the orthorhombic $(Sr_6N)[FeN_2][CN_2]_2$ and $(Sr_6N)[CoN_2][CN_2]_2$ (Table 2).

Table 2. Comparison of unit cell parameter and axis ratios for $(Sr_6N)[MN_2][CN_2]_2$ (M = Fe, Co, Cu).

	M = Fe [28]	M = Co [27]	M = Cu
Space group	$P2_12_12$ (no. 18)	$P2_12_12$ (no. 18)	$P2_1/c$ (no. 14)
Z	2	2	2
a /Å	9.938(2)	9.8807(6)	3.8454(1)
b /Å	14.717(3)	14.6474(9)	9.9244(3)
c /Å	3.856(1)	3.8569(3)	14.6528(5)
Volume *V* /Å^3	564.0	558.2	558.76
a/*b*	0.6753	0.6746	0.3874
b/*c*	3.8167	3.7977	0.6773
c/*a*	0.3880	0.3903	3.8105

A close inspection of the symmetry elements of both structures was also conducted, to see if one space group is higher in symmetry than the other. Both the space groups of $(Sr_6N)[CuN_2][CN_2]_2$, $P2_1/c$ (no. 14), and $(Sr_6N)[MN_2][CN_2]_2$ (M = Fe, Co), $P2_12_12$ (no. 18),[27,28] are subgroups of space group *Pbam* (no. 55) and both require a *translationengleiche*, *t*2, symmetry reduction from this supergroup to the either of the resultant subgroups. While both undergo the respective symmetry reduction, the monoclinic space group, $P2_1/c$ (no. 14), remains centrosymmetric, along with the screw axis and glide plane of the supergroup. In contrast, the orthorhombic subgroup, $P2_12_12$ (No. 18), maintains the orthorhombic crystal system, as well as all screw and rotational axes. Both subgroups possess different kinds of symmetry operations, but appear to have the same symmetry density, due to the near identical cell volumes.

Since no chemical or crystallographic reason could explain the variance in the crystal structure, a look into the structural complexity of each crystal structure, based on the diversity of atomic sites within the reduced unit cell, could determine if one of the structures was more complex, meaning lower in symmetry, than the other. Utilising a series of equations, based on the Shannon information theory, the complexity of the structures for $(Sr_6N)[CuN_2][CN_2]_2$ and $(Sr_6N)[MN_2][CN_2]_2$ (M = Fe, Co) could be quantitatively evaluated [Equation (1) and Equation (2)], where ρ_{inf} is the information density, v the

number of atoms in the unit cell, k the number of Wyckoff positions, ρ_i the probability of occurrence of an atom of the ith crystallographic multiplicity, and m_i the multiplicity value of the highest Wyckoff position.[43,44] For structures that have very similar unit cells, but different space groups, the one with the highest information density, and hence complexity, is the one with the lowest symmetry.

$$\rho_{inf} = \frac{-v\sum_{i=1}^{k} p_i \log_2 p_i}{V} \quad (1)$$

$$\rho_i = \frac{m_i}{v} \quad (2)$$

The density of information for $(Sr_6N)[CuN_2][CN_2]_2$ was calculated to be 0.1503 bits per Å^3 and for $(Sr_6N)[MN_2][CN_2]_2$ (M = Fe, Co) to be 0.1489 bits per Å^3 and 0.1505 bits per Å^3 respectively. Comparison of these values show that the density of information for $(Sr_6N)[CuN_2][CN_2]_2$ is higher than for $(Sr_6N)[FeN_2][CN_2]_2$, but only slightly lower than for $(Sr_6N)[CoN_2][CN_2]_2$. While the monoclinic $(Sr_6N)[CuN_2][CN_2]_2$ has a marginally lower density than $(Sr_6N)[CoN_2][CN_2]_2$, implying that $(Sr_6N)[CuN_2][CN_2]_2$ is the least complex structure, it should be noted that all of the mentioned compounds have the same number of atoms and Wyckoff positions occupied. This means that the only variable between each compound is the volume. Since there is such an extremely small variance between $(Sr_6N)[CuN_2][CN_2]_2$ and $(Sr_6N)[CoN_2][CN_2]_2$, the difference in the values of density of information between them arises solely from the differences in volume and appears to lie within the standard deviations of the unit cell determination.

Raman Spectroscopy

The Raman spectrum (Figure 4) of a red single crystal of $(Sr_6N)[CuN_2][CN_2]_2$ showed characteristic vibrational frequencies for the $[CN_2]^{2-}$ anions (Table 3). The observed symmetric stretching (ν_1 = 1232 and 1245 cm^{-1}), asymmetric stretching (ν_3 = 1949 and 1993 cm^{-1}) and deformation vibration frequencies (δ = 605 and 661 cm^{-1}) are in agreement with those observed for $(Sr_6N)[CoN_2][CN_2]_2$ (ν_1 = 1240 cm^{-1}, ν_2 = 1950 and 1978 cm^{-1} and δ = 663 and 676 cm^{-1}).[27] The measured vibrational frequencies were further confirmed to arise from $[CN_2]^{2-}$ ions through comparison with several cyanamides and carbodiimides (Table 3), while particularly the intense stretching vibrations for other three atomic linear ions as, for example, $[C_2N]^{3-}$ are located at significantly deviating (lower) wave numbers.[36–39,45]

The symmetric, asymmetric, and deformation vibrational frequencies agree well with what has been previously observed for $[CN_2]^{2-}$ anions via Raman spectroscopy.[5,11,42] The splitting at roughly 2000 cm^{-1} is typically seen for cyanamides, but is also seen in multi-cationic carbodiimides.[46] A vibrational frequency is observed at 743 cm^{-1}, which belongs to a C=N double bond, and would suggest the presence of carbodiimide rather than cyanamide ions is more probable.

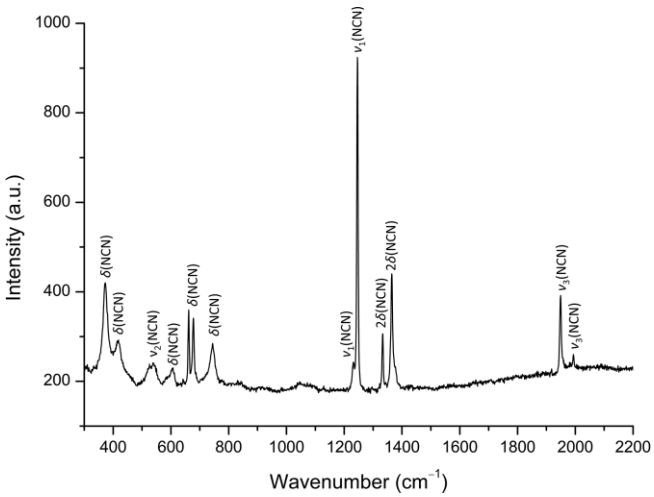

Figure 4. Raman spectrum of a single crystal of $(Sr_6N)[CuN_2][CN_2]_2$, measured using a red laser (λ = 638 nm).

Table 3. Vibrational frequencies from the Raman spectrum of $(Sr_6N)[CuN_2][CN_2]_2$. Relative intensity is denoted by the following descriptions: very strong (vs) ≥ 90 %, medium (m) 70–30 % and weak (w) 30–10 %.

Raman signal /cm^{-1}	Assignment
372 m	δ(C≡N)
418 m	δ(C≡N)
525 w	ν_2(NCN)
537 w	ν_2(NCN)
605 w	δ(NCN)
661 m	δ(NCN)
678 m	δ(NCN)
743 m	δ(C=N)
1232 w	ν_1(NCN)
1245 vs	ν_1(NCN)
1332 m	2δ(NCN)
1364 m	2δ(NCN)
1949 m	ν_3(NCN)
1993 w	ν_3(NCN)

Magnetic Susceptibility

A red single crystal was examined in a temperature range of between 5–300 K under a homogeneous magnetic field of 50 kOe (Figure S1, Supporting Information). The measurement showed the sample exhibits diamagnetic behavior. This fits with what would be expected for a sample containing Cu(I) cations, which have a completely filled 3d^{10} orbital.

Conclusions

In summary, red rectangular crystals of $(Sr_6N)[CuN_2][CN_2]_2$ were produced, which crystallize in the monoclinic space group $P2_1/c$. Single crystal diffraction refinement data identified that the crystal structure is very similar to those of $(Sr_6N)[MN_2][CN_2]_2$ (M = Fe, Co). Through Raman spectroscopy the suspected $[CN_2]^{2-}$ anions were not only confirmed, but also identified as being carbodiimide anions, which was further reinforced by the near equal C–N interatomic distances and the small anisotropic displacement parameter of

carbon atoms in the structure refinement results. The material was shown to be diamagnetic, as expected for a $3d^{10}$ system. Although structurally very similar to the other transition metal containing orthorhombic compounds $(Sr_6N)[MN_2][CN_2]_2$ (M = Fe, Co), the titular product is monoclinic and the orientation of the $[CN_2]^{2-}$ anions are noticeably different. After thorough investigations, no chemical, structural or magnetic effect could give a simple explanation for this difference.

Experimental Section

Due to the reactivity of the materials, all operations were conducted under inert conditions ($O_2 \leq 0.1$ ppm) in an argon-filled glovebox (MBraun, Garching, Germany).

Rods of elemental lithium (0.980 g, Chemetall) had the outer surface removed, using a knife, to ensure no oxides were present. The rod was cut into pieces approximately 5 mm in length. All pieces were placed into a tantalum crucible and then into a silica tube. The tube was heated under nitrogen (Alphagaz, 99.999 %) flow, which was purified by passing over a molecular sieves (4 Å) and a BTS catalyst, at 443 K for 36 hours, before increasing the temperature to 498 K at 10 K·h^{-1} for 2 h to complete the reaction. The system was then allowed to cool to room temperature. This resulted in single-phase α-Li_3N, which was confirmed by powder X-ray diffraction. A thoroughly grounded mixture of this product and Cu powder (abcr), with a molar ratio of 5:2 respectively, was pressed into a tablet weighing 1.686 g, with a diameter of 8 mm. The mixture was placed in a silica tube and heated, under nitrogen flow, to 773 K for 120 hours and then the temperature was increased to 973 K, at 50 K·h^{-1}, for 8 h, before being allowed to cool to room temperature.[47] This produced Li_2[(Li,Cu)N], which was confirmed to be single phase by powder X-ray diffraction. Determination of the amount of Cu substitution was determined via correlation between the unit cell parameters and amount of Cu.[47,48] The refined unit cell parameters [a = 3.6626(3) Å and c = 3.7928(3) Å] confirmed the actual chemical formula to be $Li_{2.6}Cu_{0.4}N$.

$Li_{2.6}Cu_{0.4}N$ (0.070 g, 1.16 mmol), elemental Sr (99.99 %, Sigma Aldrich, 0.114 g, 1.16 mmol), and C powder (99.9995 %, Alfa Aesar, 0.0058 g, 0.48 mmol) were mixed and filled in a Nb ampoule, along with elemental Na (99 %, Riedel-de-Haën, 0.120 g) as a fluxing agent. The ampoule was then sealed by an arc welder and inserted into a fused silica tube, which was then heated, under Ar flow, to 1073 K and allowed to cool at a controlled rate of 1 K·h^{-1}. After opening the ampoule, the Na flux was removed using liquid ammonia leaving a sample containing a mixture of black powder and large rectangular red crystals.

Single Crystal X-ray Diffractometry: Diffraction experiments on single crystals were carried out using a Kappa-CCD Bruker-Nonius diffractometer (Mo-K_α radiation, λ = 0.71073 Å) and the obtained data was analysed by the ShelX software package.[49]

Further details of the crystal structure investigations may be obtained from the Fachinformationszentrum Karlsruhe, 76344 Eggenstein-Leopoldshafen, Germany (Fax: +49-7247-808-666; E-Mail: crysdata@fiz-karlsruhe.de, http://www.fiz-karlsruhe.de/request for deposited data.html) on quoting the depository number CSD-1947838.

Powder X-ray Diffractometry: Powder samples of each experiment were measured using a STOE & CIE STADI P X-ray diffractometer with a Mythen1K micro-strip detector (Mo-$K_{\alpha 1}$ wavelength, λ = 0.7093 Å). Analysis of the resulting diffraction patterns were conducted using WinXPow and the Fullprof suite.[50,51]

Raman Spectroscopy: Raman spectroscopy was measured, between 10 and 2200 cm^{-1}, with an Olympus confocal polarization microscope BX51, using a red laser (λ = 638 nm). A single red rectangular crystal of the product was inserted and sealed in a glass capillary, to prevent the sample reacting with air.

Magnetic Susceptibility Measurements: Measurements of the magnetic susceptibility were conducted on a Magnetic Property Measurement System (MPMS3, Quantum Design, San Diego, USA). The red single crystal of $(Sr_6N)[CuN_2][CN_2]_2$, approximately 0.5 mm in diameter, was sealed in a glass capillary, with 0.1 mm diameter, and fixed to a plastic tube, which is typically used for these magnetic measurements, before being attached onto the sample holder of a vibrating sample magnetometer (VSM) for measuring the magnetization.

Supporting Information (see footnote on the first page of this article): Positional and displacement parameters from crystal structure refinements and temperature dependence of magnetic susceptibility

Acknowledgements

We thank *Falk Lissner* for single crystal diffraction data collection, *Manuel Häßner* for magnetic susceptibility measurements, *Adrian Geyer* for Raman spectroscopy and *Sabine Strobel* for crystallographic advice.

Keywords: Carbodiimide; Raman spectroscopy, Structure determination; Nitridometalate; Crystal growth

References

[1] A. Frank, N. Caro, *Ger. Pat.* **1895**, 88363.
[2] U. Berger, W. Schnick, *J. Alloys Compd.* **1994**, *206*, 179–184.
[3] O. Reckeweg, F. J. DiSalvo, *Z. Anorg. Allg. Chem.* **2003**, *629*, 177–179.
[4] W. Liao, R. Dronskowski, *Acta Crystallogr., Sect. E* **2004**, *60*, 124–126.
[5] K. B. Sterri, C. Besson, A. Houben, P. Jacobs, M. Hoelzel, R. Dronskowski, *New J. Chem.* **2016**, *40*, 10512–10519.
[6] X. Liu, M. Krott, P. Müller, C. Hu, H. Lueken, R. Dronskowski, *Inorg. Chem.* **2005**, *44*, 3001–3003.
[7] X. Liu, L. Stork, M. Speldrich, H. Lueken, R. Dronskowski, *Chem. Eur. J.* **2009**, *15*, 1558–1561.
[8] M. Krott, X. Liu, B. P. T. Fokwa, M. Speldrich, H. Lueken, R. Dronskowski, *Inorg. Chem.* **2007**, *46*, 2204–2207.
[9] X. Liu, M. A. Wankeu, H. Lueken, R. Dronskowski, *Z. Naturforsch. B* **2005**, *60*, 593–596.
[10] M. Becker, M. Jansen, *Acta Crystallogr., Sect. C* **2001**, *57*, 347–348.
[11] G. Baldinozzi, B. Malinowska, M. Rakib, G. Durand, *J. Mater. Chem.* **2002**, *12*, 268–272.
[12] R. K. Zheng, H. Liu, Y. Wang, X. X. Zhang, *J. Appl. Phys.* **2004**, *96*, 5370–5372.
[13] M. Jansen, M. Becker, *Z. Anorg. Allg. Chem.* **2000**, 1639–1641.
[14] X. Liu, P. Müller, P. Kroll, R. Dronskowski, *Inorg. Chem.* **2002**, *41*, 4259–4265.
[15] M. T. Sougrati, A. Darwiche, X. Liu, A. Mahmoud, R. P. Hermann, S. Jouen, L. Monconduit, R. Dronskowski, L. Stievano, *Angew. Chem. Int. Ed.* **2016**, *55*, 5090–5095.
[16] A. Eguía-Barrio, E. Castillo-Martínez, X. Liu, R. Dronskowski, M. Armand, T. Rojo, *J. Mater. Chem. A* **2016**, *4*, 1608–1611.

[17] C. Liu, C. Zhang, H. Fu, X. Nan, G. Cao, *Adv. Energy Mater.* **2017**, *7*, 1601127.
[18] A. Eguia-Barrio, E. Castillo-Martinez, X. Liu, R. Dronskowski, L. Lezama, M. Armand, T. Rojo, *MRS Adv.* **2017**, *2*, 1165–1176.
[19] A. Eguia-Barrio, E. Castillo-Martínez, F. Klein, R. Pinedo, L. Lezama, J. Janek, P. Adelhelm, T. Rojo, *J. Power Sources* **2017**, *367*, 130–137.
[20] J. Sinko, *Patent-US6139610A*, **1998**.
[21] Q. Liu, Y. Liu, G. Dai, L. Tian, J. Xu, G. Zhao, N. Zhang, Y. Fang, *Appl. Surf. Sci.* **2015**, *357*, 745–749.
[22] M. Kubus, R. Heinicke, M. Ströbele, D. Enseling, T. Jüstel, H. J. Meyer, *Mater. Res. Bull.* **2015**, *62*, 37–41.
[23] M. Kubus, C. Castro, D. Enseling, T. Jüstel, *Opt. Mater.* **2016**, *59*, 126–129.
[24] M. Krings, G. Montana, R. Dronskowski, C. Wickleder, *Chem. Mater.* **2011**, *23*, 1694–1699.
[25] S. Yuan, Y. Yang, F. Chevire, F. Tessier, X. Zhang, G. Chen, *J. Am. Chem. Soc.* **2010**, *132*, 3052–3055.
[26] R. Dronskowski, S. Kikkawa, A. Stein, *Handbook of Solid State Chemistry*, Wiley-VCH Verlag GmbH & Co. KGaA, Weinheim, Germany, **2017**.
[27] J. K. Bendyna, P. Höhn, W. Schnelle, R. Kniep, *Sci. Technol. Adv. Mater.* **2007**, *8*, 393–398.
[28] J. K. Bendyna, P. Höhn, R. Kniep, *Z. Kristallogr.* **2009**, *224*, 5–6.
[29] P. Höhn, R. Kniep, *Z. Anorg. Allg. Chem.* **2002**, *628*, 2173.
[30] O. Reckeweg, F. J. DiSalvo, *Z. Naturforsch. B* **2003**, *58*, 201–204.
[31] J. K. Bendyna, P. Höhn, Y. Prots, R. Kniep, *Z. Anorg. Allg. Chem.* **2010**, *636*, 1297–1300.
[32] W. Clark, R. Niewa, *Crystals* **2018**, *8*, 268.
[33] R. Niewa, H. Jacobs, *Chem. Rev.* **1996**, *96*, 2053–2062.
[34] H. Yamane, F. J. DiSalvo, *Prog. Solid State Chem.* **2018**, *51*, 27–40.
[35] R. Niewa, F. J. DiSalvo, *J. Alloys Compd.* **1998**, *279*, 153–160.
[36] H. Womelsdorf, H.-J. Meyer, *Z. Anorg. Allg. Chem.* **1994**, *620*, 262–265.
[37] W. P. Clark, R. Niewa, *submitted*.
[38] F. Jach, S. I. Brückner, A. Ovchinnikov, A. Isaeva, M. Bobnar, M. F. Groh, E. Brunner, P. Höhn, M. Ruck, *Angew. Chem. Int. Ed.* **2017**, *56*, 2919–2922.
[39] F. Jach, P. Höhn, Y. Prots, M. Ruck, *Eur. J. Inorg. Chem.* **2019**, *2019*, 1207–1211.
[40] R. Juza, H. Hahn, *Z. Anorg. Allg. Chem.* **1938**, *239*, 282–287.
[41] U. Zachwieja, H. Jacobs, *J. Less-Common Met.* **1990**, *161*, 175–184.
[42] A. Wosylus, U. Schwarz, L. Akselrud, M. G. Tucker, M. Hanfland, K. Rabia, C. Kuntscher, J. von Appen, R. Dronskowski, D. Rau, R. Niewa, *Z. Anorg. Allg. Chem.* **2009**, *635*, 1959–1968.
[43] C. E. Shannon, W. Weaver, *The Mathematical Theory of Communication*, Univ. of Illinois Press, **1963**.
[44] S. V. Krivovichev, *Angew. Chem. Int. Ed.* **2014**, *53*, 654–661.
[45] M. Somer, U. Herterich, J. Čurda, W. Carrillo-Cabrera, A. Zürn, K. Peters, G. von Schnering, *Z. Anorg. Allg. Chem.* **2000**, *626*, 625–633.
[46] A. J. Corkett, P. M. Konze, R. Dronskowski, *Z. Anorg. Allg. Chem.* **2017**, *643*, 1456–1461.
[47] Z. Stoeva, R. Gomez, D. H. Gregory, G. B. Hix, J. J. Titman, *Dalton Trans.* **2004**, 3093–3097.
[48] R. Niewa, Z.-L. Huang, W. Schnelle, Z. Hu, R. Kniep, *Z. Anorg. Allg. Chem.* **2003**, *629*, 1778–1786.
[49] a) *G. M. Sheldrick*, Program SHELX-97, **1997**; b) *Stoe & Cie GmbH*, Program X-RED 32, **2005**; c) *Stoe & Cie GmbH*, Program X-STEP 32, **2000**; d) *Stoe & Cie GmbH*, Program X-SHAPE 32, **1999**.
[50] *Stoe & Cie GmbH*, Program WINXPOW, **2001**.
[51] *Fullprof Team*, Program Fullprof Suite, **2011**.

Received: September 10, 2019
Published Online: November 19, 2019

